arXiv:cond-mat/0307450v1 [cond-mat.supr-con] 18 Jul 2003

Probing quasiparticle dynamics in $Bi_2Sr_2CaCu_2O_{8+\delta}$ with a driven Josephson vortex lattice

Yu. I. Latyshev
Institute of Radio-Engineering and Electronics, Russian Academy of Sciences, Mokhovaya 11-7, 101999 Moscow, Russia

A. E. Koshelev
Materials Science Division, Argonne National Laboratory, Argonne, Illinois 60439

L. N. Bulaevskii
Los Alamos National Laboratory, Los Alamos, NM 87545, USA

We show that the flux-flow transport of the Josephson vortex lattice (JVL) in layered high-temperature superconductors provides a convenient probe for both components of quasiparticle conductivity, σ_c and σ_{ab}. We found that the JVL flux-flow resistivity, ρ_{ff}, in a wide range of magnetic fields is mainly determined by the in-plane dissipation. In the dense lattice regime ($B > 1$ T) $\rho_{ff}(B)$ dependence is well fitted by the theoretical formula for that limit. That allows us to independently extract from the experimental data the values of σ_c and of the ratio $\sigma_{ab}/(\sigma_c\gamma^4)$. The extracted temperature dependence $\sigma_{ab}(T)$ is consistent with microwave data. The shape of the current-voltage characteristics is also sensitive to the frequency dependence of σ_{ab} and that allows us to estimate the quasiparticle relaxation time and relate it to the impurity bandwidth using data obtained for the same crystal.

I. INTRODUCTION

The properties of quasiparticles (QPs) in the high-temperature cuprate superconductors are unusual due to d-wave gapless pairing in these systems. The concentration of QPs in clean d-wave superconductors vanishes in the limit $T \to 0$ because their density of states (DOS) has asymptotics $\rho(\epsilon) \propto \epsilon$ at low energies, $\epsilon \to 0$. Such d-wave features of the QPs spectrum has been clearly demonstrated by angular-resolved photoemission (ARPES) studies (see, e. g., Refs. 1) and confirmed by numerous transport measurements. However, QP transport properties are still in the focus of hot debate and new experimental techniques are very valuable in understanding of these properties. In this paper we use the driven Josephson vortex lattice to probe both in-plane and inter-plane QP transport and compare results with other techniques.

We start with brief overview of the QP physics in the high-temperature superconductors. The main issues are how impurities modify the QPs spectrum and how they affect mobility of the QPs. Two competing effects determine QP transport at low temperatures. It was recognized very early that impurities in unconventional superconductors destroy the superconducting order parameter in their vicinity increasing the DOS at low energies.[2] This effect enhances the low-temperature QP transport. On the other hand, increase the QPs scattering rate by impurities suppresses the QP transport. In addition, there is a tendency for QPs localization due to the two-dimensionality of superconducting CuO_2 layers.

The low-energy asymptotics of the QP DOS in inhomogeneous d-wave superconductors is a challenging theoretical problem, which is not settled yet. Several approximations have been used to calculate $\rho(\epsilon)$ leading to different results. In the self-consistent T-matrix approximation (SCTMA)[3,4,5] the DOS approaches a finite value $\rho(\epsilon) \approx \rho(0)$ for $\epsilon \lesssim \gamma_i$ and $\rho(\epsilon) \propto \epsilon$ for $\epsilon > \gamma_i$, where the impurity bandwidth γ_i depends on the impurity concentration and the impurity potential. In the limit of strong impurity potential (unitary limit) one gets for the impurity bandwidth[3] $\gamma_i \approx (\hbar\nu_0\Delta_0)^{1/2}$, where ν_0 is the normal-state relaxation rate and Δ_0 is the magnitude of the superconducting gap.

With $\rho(\epsilon)$ known, the QPs transport can be calculated in the framework of the Fermi liquid theory. Along this line Lee[3] predicted a universal (impurity independent) low-temperature limit for the intralayer electrical conductivity, $\sigma_{00}^{(ab)} = ne^2/(\pi m_{ab}\Delta_0)$, arguing that both, the DOS and the scattering rate are proportional to the impurity concentration and thus cancel in the Drude expression for the conductivity. Here n is the carrier concentration and m_{ab} is the QP in-plane effective mass. In the same way universal thermal conductivity was predicted by Sun and Maki[6] and by Graf *et al.*[7] Later it was shown in Refs. 8 that electron interactions inside the layers lead to the Fermi-liquid corrections to the universal electrical conductivity. Durst and Lee[9] found that such corrections as well as the asymmetric scattering (i.e. the difference between the QPs relaxation rate and the transport scattering rate) result in the expression for the intralayer electrical conductivity $\sigma_{ab}(T) = \sigma_{00}^{(ab)}\beta$. Experimentally observed values of low-temperature σ_{ab} usually correspond to $\beta > 1$, see Ref. 10. Durst and Lee found also that such corrections to the universal thermal conductivity at $\epsilon \lesssim \gamma_i$ are practically absent.

For the interlayer tunneling conductivity, σ_c, in highly anisotropic layered cuprates like BSCCO the authors of Ref. 11 have argued that it is universal in the limit of low impurity concentration, when electrons tunnel be-

tween layers conserving their in-plane quasi-momentum (coherently). In contrast to σ_{ab}, σ_c depends only on the intralayer DOS (i.e., on the QPs relaxation rate). It is not sensitive to anisotropy of the in-plane scattering and in-plane vertex corrections are not important. In this case the low-temperature conductivity $\sigma_{00}^{(c)}$ is related to the Josephson critical current density $J_c(0)$ by a simple relation similar to the well-known Ambegaokar-Baratoff relation in conventional Josephson junctions, $\sigma_{00}^{(c)} = 2esJ_c(0)/(\pi\Delta_0)$, where s is the interlayer spacing. In the framework of SCTMA-Fermi-liquid approach the temperature corrections to the universal conductivity $\sigma_{00}^{(c)}$ at $T < \gamma_i$ were found[11] to be

$$\sigma_c(T) \approx \sigma_{00}^{(c)}[1 + (\pi T)^2/18\gamma_i^2]. \quad (1)$$

A similar result has been obtained for the in-plane QP conductivity neglecting anisotropic scattering and vertex corrections.[5] However, it is known that such corrections substantially modify $\sigma_{ab}(T)$. For the thermal conductivity, $\kappa(T)/T$, in the unitary limit, the thermal corrections are also quadratic in T/γ_i, as for σ_c, and only in the limited temperature interval linear in T corrections were found if the impurity potential is not very strong.[12]

The more elaborate approaches, which take into account interference effects, suggest that the QP DOS vanishes at $\epsilon \to 0$ (see recent review in Ref. 13). In particular, recent numerical analysis[14] have demonstrated that QP DOS behaves at very low energies as $\rho(\epsilon) \propto \epsilon^\alpha$ with a nonuniversal exponent α. This exponent depends on the details of disorder model and particle-hole symmetry in the normal state. In the realistic case (binary alloy model without particle-hole symmetry) they found $\alpha > 0$, i.e., a DOS suppression at low energies. The energy scale for this suppression is given is the resonance energy for an isolated impurity Ω_0 with $\Omega_0 \to 0$ as the impurity potential increases. This means that at very low temperatures, $T \ll \Omega_0$, QP transport should vanish.

Intralayer conductivity was studied by a microwave technique[10,15,16,17] and infrared spectroscopy.[18,19,20] These measurements have shown that $\sigma_{ab}(T)$ is not universal in the low temperature limit and that its temperature dependence at $T \sim \gamma_i$ deviates strongly from SCTMA predictions,[5] see below. The impurity bandwidth can be estimated from the frequency dependence of the intralayer conductivity, $\sigma_{ab}(\omega)$. According to the model calculation of Ref. 5, the typical relaxation rate, $1/\tau$, in $\sigma_{ab}(\omega)$ has to be of the order of γ_i. Recent terahertz spectroscopy measurements of $\sigma_{ab}(\omega)$ in $Bi_2Sr_2CaCu_2O_{8+\delta}$ (BSCCO) by Corson *et al.*[17] showed that at low temperatures it has a Drude frequency dependence with the typical relaxation rate $1/\tau \approx 1$ THz. This gives an estimate $\gamma_i = 30 - 50$K.

Experimentally a universal value of κ_{00}/T was confirmed by measurements[21,22,23] of the thermal conductivity in BSCCO and YBCO crystals. Particularly, Nakamae *et al.*[22] measured thermal conductivity in pristine and irradiated BSCCO crystals at $T < 0.1$ K. Direct comparison of $\kappa(T)$ in pristine and irradiated crystals showed almost the same value κ_{00}/T obtained by extrapolation to $T = 0$. However, strong temperature corrections, linear in T, to this universal value were found below 0.25 K. Such corrections are not anticipated well below $\gamma_i \approx 20$ K in the SCTMA approach. One can conclude from these measurements, that the upper limit for the low temperature behavior, Ω_0, lies below 0.1 K and that temperature behavior of $\kappa(T)$ observed so far is in contradiction with the theoretical SCTMA predictions.

Measurements of interlayer conductivity seems to follow closely to the theoretical predictions of the the SCTMA-Fermi-liquid model assuming coherent interlayer tunneling.[11] For BSCCO crystals from different groups, similar values, $\sigma_{00}^{(c)} \approx 2$ [k$\Omega\cdot$ cm]$^{-1}$ were observed by measurements of the I-V characteristics, though universality of this value was not checked by comparison of crystals before and after irradiation as it was done for the thermal conductivity.[22] The temperature dependence of $\sigma_c(T)$ at $T < \gamma_i$ was found to be in agreement with the theoretical prediction, Eq. (1), and the values of γ_i in the interval 24-29 K were derived from fitting, in agreement with the data for the relaxation rate τ mentioned above.

The intralayer and interlayer components of the QP conductivity are found to have qualitatively different temperature dependencies in the superconducting state. The interlayer conductivity monotonically decreases with temperature decrease in the whole temperature range from T_c down to lowest temperatures. In contrast, the intralayer conductivity has manifestly nonmonotonic behavior: it rapidly *increases* with decrease of temperature in some region below T_c reaches a peak at some intermediate temperature, and decreases with further decrease of temperature.[10,15,16,17] This behavior is also consistent with the heat transport measurements for the electronic part of the thermal conductivity.[23] The peak in the temperature dependence of σ_{ab} appears due to an interplay between the temperature dependencies of the relaxation rate[17] and concentration of quasiparticles. The unusual increase of the QP conductivity and thermal conductivity just below T_c is attributed to the fast drop of the relaxation rate due to the reduction of the phase space for scattering.[12] Decrease of the conductivity at low temperatures, below the peak, is caused by a drop in the concentration of the thermally activated nodal quasiparticles.

Hence, the behavior of QPs in the cuprate d-wave superconductors is not fully understood yet and new methods to probe the QP transport would be useful to resolve controversy and provide additional information on the characteristic parameters, such as Ω_0.

Recently a new method of probing the QP conductivities σ_c and σ_{ab} has been suggested.[24] The method is based on the measuring of the losses, associated with a transport of the Josephson vortex lattice (JVL)[25] driven by steady current across the layers in crystals with intrinsic Josephson interlayer coupling.[26] The unexpected dependence of the interlayer transport on the intralayer

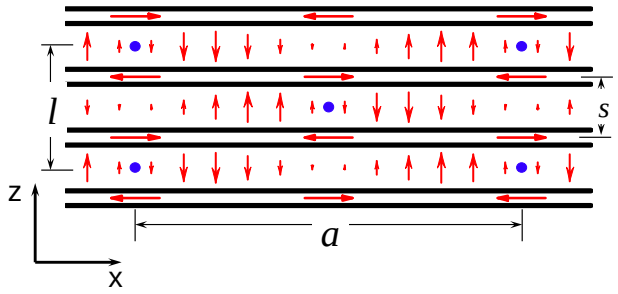


FIG. 1: Dense Josephson vortex lattice with period $l = 2s$ in the c-direction. Arrows show the direction of currents.

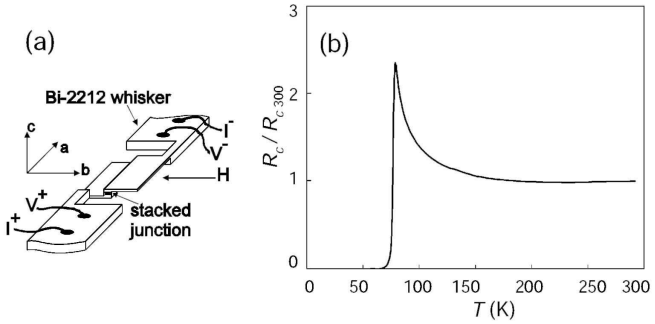


FIG. 2: (a)Schematic view of junction orientation and experimental set up. (b)Normalized temperature dependence of resistance along the c-axis of typical long stacked junction used in experiment.

quasiparticle conductivity in the flux-flow regime is related to the spatially inhomogeneous structure of moving JVL. Figure 1 shows the space structure of a stationary high-field Josephson lattice.[25] Inside the layers the supercurrent oscillates along the direction perpendicular to the applied parallel magnetic field (x -axis). The interlayer transport current drives the vortex lattice along the x-axes. At small velocities the lattice is practically undistorted. Then the supercurrent inside the layer at a given point changes periodically with time, $j_{sx} \propto \sin(2\pi vt/a)$, where v is the lattice velocity and $a = \Phi_0/sH$ is the period of vortex lattice. According to the first London equation (see, e.g., Ref. 27)

$$E_x = \frac{4\pi\lambda_{ab}^2}{c^2}\frac{\partial j_{sx}}{\partial t}, \quad \lambda_{ab}^2 = \frac{m_{ab}c^2}{4\pi n_s e^2},$$

an alternating electric field E_x with frequency $\omega = 2\pi v/a$ is introduced by a moving vortex lattice. Here n_s is the density of superconducting electrons. The electric field causes relaxation due to quasiparticle current $j_{qx} = \sigma_{ab}E_x$. Hence, as was shown, both components of the QP conductivity σ_c and σ_{ab} contribute to the Josephson flux-flow resistivity ρ_{ff} and can be extracted separately from the magnetic field dependence of ρ_{ff}. Moreover, the shape of the I-V characteristic related to JVL motion at high magnetic fields is sensitive to the frequency dependence of the QP conductivity and therefore may be used to estimate the QP relaxation time. This approach allows one to probe the relatively low frequency range of the QP conductivity, 0.01-3 THz, and thus the results can be easily compared with the data of microwave measurements. The goal of the present paper is to demonstrate the applicability of this new method for studies of the QP conductivity in BSCCO.

Motion of JVL induced by a steady current across the layers results in a specific branch on the I-V characteristic usually referred to as the Josephson flux-flow (JFF) branch. That is characterized by a rapid current increase when the voltage approaches a certain limiting value, V_m, at which the lattice velocity approximately reaches the velocity of electromagnetic wave propagation (this velocity frequently is refered to as the Swihart velocity in analogy with a single long Josephson junction). The JFF regime is well known for conventional long Josephson junctions[28] and has also been observed on BSCCO mesa structures.[29,30,31] Our purpose was to study the JFF linear and non-linear regimes on long BSCCO stacks at high magnetic fields above 0.5 T when a dense JVL is formed. Early experiments on JFF in BSCCO have been done mostly at relatively low fields[29,31] or at high fields of only few fixed values.[30] In addition, an absence of the clear upturn curvature on JFF branch[30] suggests significant inhomogeneities in the mesas used in early experiments.

We report new measurements that allow us to obtain for the first time the parameters $1/\tau$ and γ_i for the same crystal and correlate the frequency and temperature dependencies of quasiparticle conductivities.

II. EXPERIMENTAL

To obtain high-quality stacks we fabricated samples from single crystal whiskers of BSCCO. The thin BSCCO whiskers have been characterized as extremely perfect crystalline objects[32]. They grow along the [100] direction free of any crucible or substrate and can be entirely free of macroscopic defects and dislocations. The stacks have been fabricated by the double-sided processing of the BSCCO whiskers by the focused ion beam (FIB) technique. The stages of fabrications were similar to those described in Ref. 33. Figure 2a shows schematically the geometry and orientation of the structure with respect to the crystallographic axes. We reproduced the overlap type of long stack geometry which is known to provide the most uniform current distribution along the junction.[28] The structure sizes were $L_a = 20 - 30$ μm, $L_b = 1 - 2$ μm, $L_c = 0.05 - 0.15$ μm. Using high-resolution optical microscope we selected for the experiment long uniform whiskers with a length of 500-1000 μm, a thickness of 0.5-1 μm and a width of 10-20 μm. Four silver contact pads have been evaporated and annealed at 450°C in oxygen flow before FIB processing to avoid diffusion of Ga-ions into the junction body. The fabricated structures have been then tested by $R_c(T)$ measurements to select ones

free of inclusions of 2201 or 2223 phases. The presence of these phases is indicated as a multiple transition to superconducting state with appropriate drops of $R_c(T)$ at 90-100K for 2223 phase and at 15-30K for 2201 phase. Only single-phase 2212 stacked junctions with a single transition at 75-80 K (see Fig. 2b) have been selected for the further measurements. A yield of the single-phase stacks was quite high, about 30-50%. The oxygen doping level of the stacks estimated from $\rho_c(T)$ measurements above T_c[34] was slightly above optimum, $\delta \approx 0.25$. The critical current density J_c at 4.2 K in the absence of magnetic field was 1-2 kA/cm^2. Measurements of the I-V characteristics of BSCCO stacks have been carried out in the commercial cryostat of Quantum Design PPMS facility. The magnetic field has been oriented parallel to the b-axis within accuracy 0.1° and has been changed in steps of 0.05-0.1 T. In each fixed value of the field the I-V characteristics have been measured using a fast oscilloscope. We have measured 6 samples with similar results.

III. RESULTS AND DISCUSSION

Fig. 3 shows the I-V characteristics of a long stack #4 ($30 \times 2 \times 0.14$ μm^3) at $T = 20$ K at zero magnetic field (Fig. 3a) and at the field $B = 1.5$T (Fig. 3b) oriented along the b-axis. At zero magnetic field the I-V characteristics of the stacks show a well-defined critical current shown at Fig. 3a as a vertical trace with the following switch to the multibranched structure. The I-V characteristic is highly hysteretic. The hysteresis loop is shown in Fig. 3a schematically by arrows (the first switch here corresponds to the jump from the critical current to the 4^{th} branch). Both features, the hysteresis and the multibranched structures of the I-V characteristics, are well known for Bi-2212 stacked junctions at low temperatures.[35]

In the presence of a parallel field the critical current becomes essentially suppressed and the JFF branch develops. That is characterized by a linear slope at low bias, R_{ff}, by a pronounced upturn at higher bias voltages, and by jumps to the multiple branches at the voltages exceeding the maximum value V_m. The high upturn in the nonlinear I-V characteristics in the parallel field proves a high quality of our stacks. To get the $R_{ff}(B)$ dependence we measured a set of the I-V characteristics at some temperatures for the fixed fields increasing step by step. At each field we measured R_{ff}. The value of R_{ff} has been defined as an extrapolation of the linear part of the I-V at $|V| \to 0$. As seen from Fig. 3c, this extrapolation can be easily done at high fields when critical current is highly suppressed. An accuracy of linear extrapolation of the I-V characteristic at $|V| < 10$mV for definition of R_{ff} was within 5%. Fig. 3c shows an evolution of the I-Vs with field. One can see a rapid increase of R_{ff} and V_m with field. The summarized field dependencies of R_{ff} and V_m for typical sample (#4) are shown at Figs. 4 and 5. Before analyzing these data we discuss the expected theoretical dependencies.

Firstly, we will consider the linear limit of the I-V characteristics corresponding to low JFF velocity. In the second part, we will focus on the high-velocity JFF limit.

A. Linear flux-flow resistivity.

The linear flux-flow resistivity of the Josephson vortex lattice, ρ_{ff}, is determined by the static lattice structure and linear quasiparticle dissipation. At high fields, $B > \Phi_0(\pi\gamma s^2)$, the Josephson vortices homogeneously fill all the layers and the static lattice structure is characterized by oscillating patterns of both c-axis and in-plane supercurrents[25] (see Fig. 1). Here γ is the anisotropy ratio of the London penetration lengths, $\gamma = \lambda_c/\lambda_{ab}$. At small velocities this pattern slowly drifts along the direction of layers, preserving its static structure. This motion produces oscillating c-axis ($\tilde{E}_z$) and in-plane ($\tilde{E}_x$) electric fields leading to extra dissipation, in addition to usual dissipation due to the dc electric field E_z. Total dissipation per unit volume is given by

$$\sigma_{ff} E_z^2 = \sigma_c E_z^2 + \sigma_c \left\langle \tilde{E}_z^2 \right\rangle + \sigma_{ab} \left\langle \tilde{E}_x^2 \right\rangle , \qquad (2)$$

where $\sigma_{ff} = 1/\rho_{ff}$ is the flux-flow conductivity, $\langle \ldots \rangle$ means time and space average, $\sigma_c = 1/\rho_c$ and $\sigma_{ab} = 1/\rho_{ab}$ are the c-axis and in-plane quasiparticle conductivities. An expansion with respect to the Josephson current at high fields allows to relate $\tilde{E}_z$ and $\tilde{E}_x$ with E_z,

$$\begin{aligned} \tilde{E}_{nz}(x,t) &= -(-1)^n \frac{4E_z}{h^2} \cos\left(k_H x + \omega t\right), \\ \tilde{E}_{nx}(x,t) &= (-1)^n \frac{2E_z}{\gamma h} \sin\left(k_H x + \omega t\right), \end{aligned}$$

with $h = 2\pi\gamma s^2 B/\Phi_0$ and $k_H = 2\pi s B/\Phi_0$. Here n is the layer index. Finally, we obtain a simple analytical formula for the flux-flow resistivity[24,36]

$$\rho_{ff}(B) = \frac{B^2}{B^2 + B_\sigma^2}\rho_c, \quad B_\sigma = \sqrt{\frac{\sigma_{ab}}{\sigma_c}} \frac{\Phi_0}{\sqrt{2}\pi\gamma^2 s^2}, \qquad (3)$$

The relative importance of the in-plane and c-axis dissipation channels is determined by the dimensionless ratio $\Gamma = \sigma_{ab}/(\sigma_c\, \gamma^2)$. The in-plane dissipation channel dominates when $\Gamma \gg 1$.

Experimental dependencies of the JFF resistance, $R_{ff}(B)$, on magnetic field B applied along the b-axis at various temperatures are depicted in Fig. 4. They are evidently nonlinear with the type of non-linearity predicted by Eq. (3): quadratic growth with the following saturation. As shown in Fig. 4, the data can be well fitted to Eq. (3) in the wide range of temperatures. Two fitting parameters have been used for each curve, R_c, the high field saturation value of the resistance, $R_{ff}(B)$, and the characteristic field B_σ, both defined by Eq. (3). Using

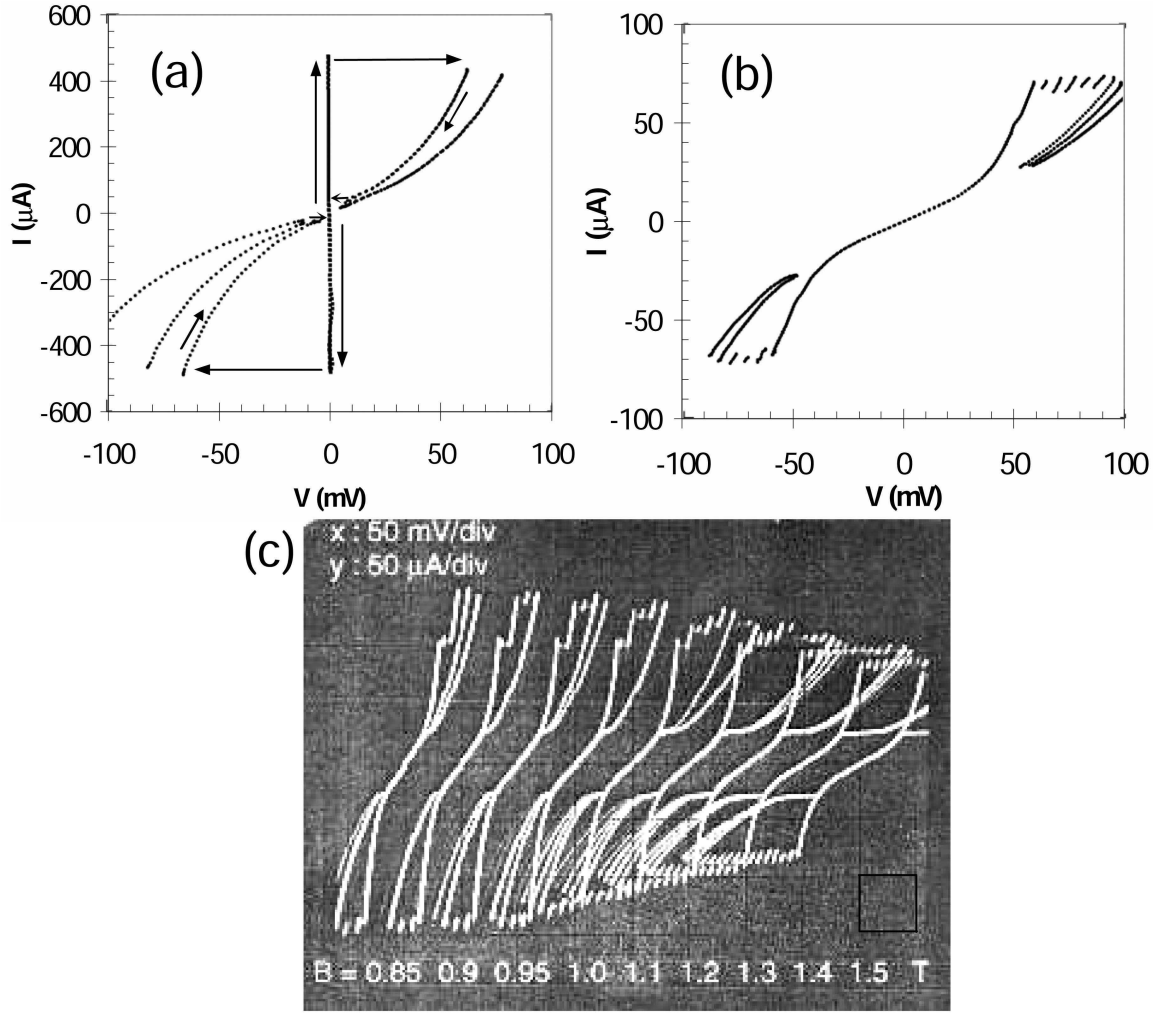


FIG. 3: The I-V characteristics of stack #4 at 4.2 K without magnetic field (a) and with field B applied along b-axis, $B = 1.5$T (b), with B increasing from 0.85 T up to 1.5 T (c). The first three branches are not traced on the I-V characteristic in zero field and the stack jumps directly to the 4th branch.

that fit at a set of temperatures we found a temperature variation of both parameters. Then, from the temperature dependence of R_c we can directly get the dependence of $\sigma_c(T)$, while the temperature dependence B_σ contains information about the ratio $\sigma_{ab}(T)/\sigma_c(T)$ for given values of γ. For T = 4.2 K we found $B_\sigma = 3.3$ T. We estimate the value of $\gamma \approx 500$ at 4.2 K from the value of the Josephson critical current density $J_c(0) = 1.7$ kA/cm^2 and the value of $\lambda_{ab}(0) = 0.2$ μm using the well-known expression[37], $J_c = c\Phi_0/(8\pi^2 s\gamma^2\lambda_{ab}^2)$. That gives a quite reasonable value for σ_{ab} at 4.2 K, $\sigma_{ab}(4.2) = 4\cdot 10^4$ (Ohm cm)$^{-1}$. Finally, we restored the temperature dependence of the in-plane quasiparticle conductivity $\sigma_{ab}(T)$ taking into account the temperature dependence of γ. We used the $\gamma(T)$ dependence extracted from the known data for $\lambda_{ab}(T)$[38] and $\lambda_c(T)$[39] in BSCCO. Actually, γ^2 only weakly depends on T, slowly decreasing within 15%, with temperature increase from 4.2 to 70 K.

Figure 6 demonstrates the temperature dependencies of σ_{ab} and σ_c extracted from the Josephson flux-flow experiment. As we found, σ_{ab} rapidly increases below T_c with decrease of T, reaches a maximum at about 30K, and then drops down at low temperatures. That type of $\sigma_{ab}(T)$ behavior has been found earlier in the microwave experiments for YBCO[26] and BSCCO[15,16,17] and also is consistent with the heat transport measurements of the electronic part of the thermal conductivity.[23] As discussed in the Introduction, the peak in the temperature dependence of σ_{ab} appears due to an interplay between the competing temperature dependencies of the relaxation rate[17] and concentration of quasiparticles. We found that the value and temperature dependence of σ_{ab} extracted from the Josephson flux-flow experiment quite well reproduce the low-frequency microwave data.[15] The sharper increase of $\sigma_{ab}(T)$ below T_c may be related to weaker scattering of the quasiparticles in the BSCCO single-crystal whiskers used in our experiments. At higher temperatures the data are also consistent with

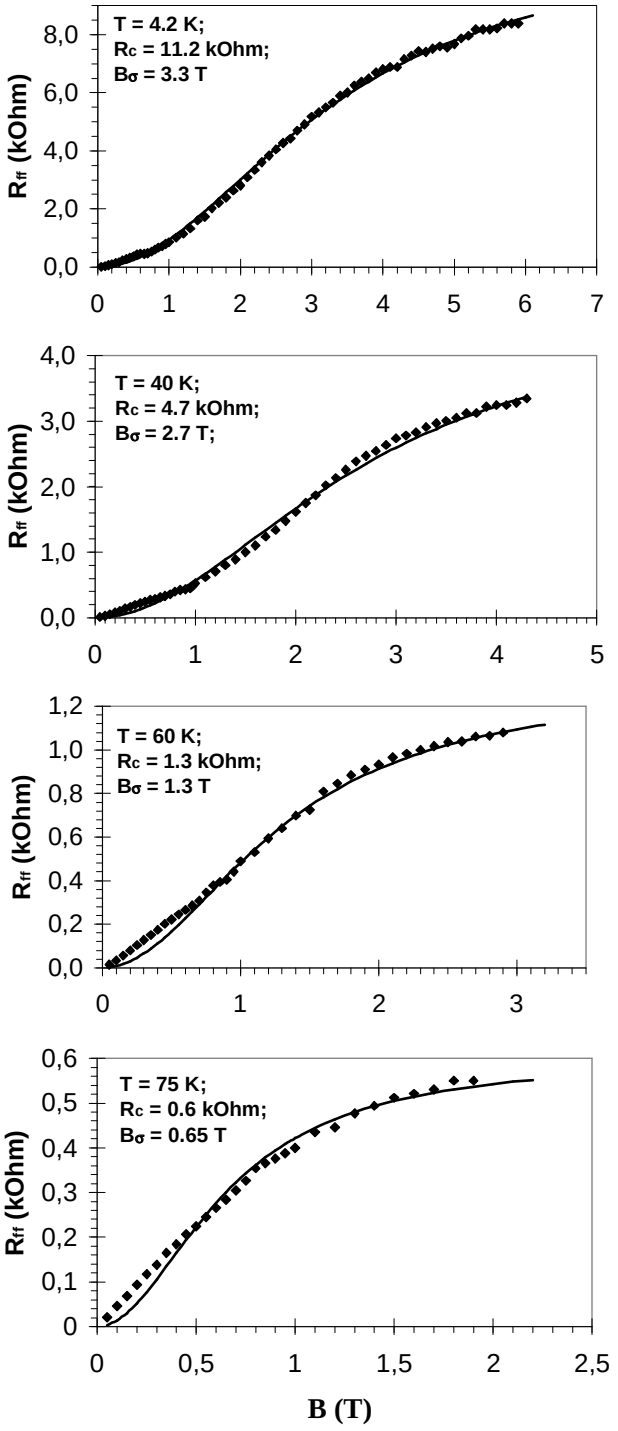


FIG. 4: Magnetic field dependence of the Josephson flux-flow resistance, R_{ff} at different temperatures with fits to Eq. (3).

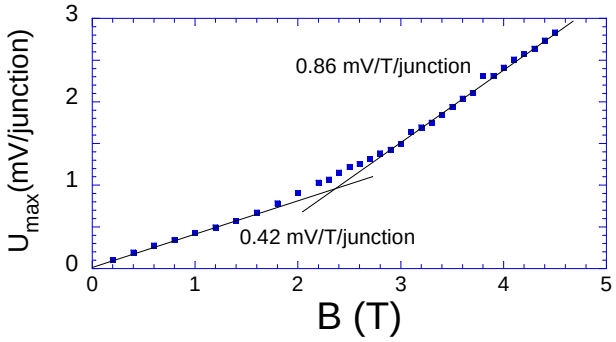


FIG. 5: Magnetic field dependence of maximum voltage of Josephson flux-flow branch, V_{max}.

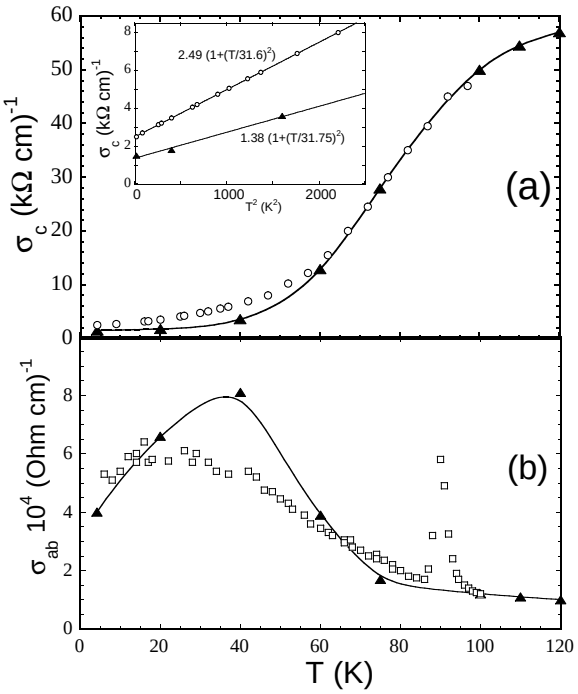


FIG. 6: Solid triangles show temperature dependencies of the out of plane quasiparticle conductivity σ_c (a) and in-plane quasiparticle conductivity σ_{ab} (b). Below T_c they extracted from the JFF experiment on BSCCO long stack #4 and above T_c they represent the *dc* normal-state conductivities of whiskers measured independently on samples from the same batch. Open circles correspond to the σ_c data from Ref. 11, obtained on small mesas in zero field, open squares correspond to 14.4 GHz microwave data for σ_{ab} from Ref. 15 obtained on BSCCO epitaxial films. Solid lines in both plots are just guides to the eye. Inset in the upper figure shows the low-temperature part of $\sigma_c(T)$ plotted versus T^2.

the results of DC measurements of $\sigma_{ab}(T)$ in the normal state carried out at the whiskers from the same batch[32] (see the points at $T \geq 100$ K). We see that, in contradiction with the naive SCTMA predictions,[5] $\sigma_{ab}(T)/\sigma_{ab}(0) - 1 \sim (T/\gamma_i)^2$, $\sigma_{ab}(T)$ has strong temperature dependence at $T < \gamma_i \approx 30$ K so that the saturation to the low-temperature value is not reached even at 4 K.

In contrast, the temperature dependence of σ_c extracted from the flux-flow experiment (Fig. 6a) is consistent with $\sigma_c(T)$ measured on small mesas in zero magnetic field,[11] with $\sigma_c(0)$ being close to the universal value $\sigma_c(0) \approx 2$ (kΩ cm)$^{-1}$ predicted in Ref. 11. The data

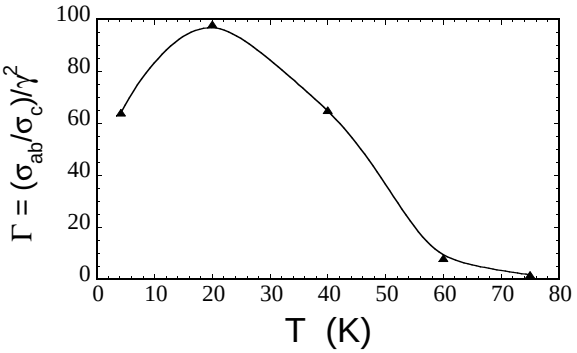


FIG. 7: Temperature dependence of the parameter $\Gamma = (\sigma_{ab}\sigma_c)/\gamma^2$. Solid line is a guide to eyes.

also well extrapolate to the points of *dc* measurements of $\sigma_c(T)$ of the same mesas in the normal state. The temperature dependence of $\sigma_c(T)$ is in agreement with the theoretical prediction Eq. (1) with $\gamma_i \approx 23.5$ K.

Clearly, behavior of $\sigma_{ab}(T)$ and $\sigma_c(T)$ is very different. This can be seen more clear in the temperature dependence of their ratio. In Fig. 7 we plot temperature dependence of the parameter $\Gamma = (\sigma_{ab}/\sigma_c)/\gamma^2$ (the ratio of the QP dissipation anisotropy to the superconducting anisotropy). The important point is that both components of the quasiparticle conductivity were extracted from the same experiment. As was mentioned above the in-plane contribution to the flux-flow resistivity becomes considerable when $\Gamma \gg 1$. Figure 7 shows that this condition is indeed valid in a wide temperature range below T_c. Note that the value of Γ approaches 1 when T approaches T_c. The value of Γ also decreases below 20 K. The interesting issue is the low-temperature limit of Γ. Without Fermi-liquid and anisotropic scattering corrections to the universal electrical intralayer conductivity, Γ should approach unity at low temperatures, $T \ll \gamma_i$, but obtained Γ is still well above unity at 4 K.

B. Nonlinear Josephson flux-flow regime.

A non-linear Josephson flux-flow occurs at high velocities of Josephson vortex lattice, especially at velocities approaching the minimum velocity of the electromagnetic wave (Swihart velocity), $c_s = cs/(2\lambda_{ab}\sqrt{\epsilon})$. The main source of the nonlinearity is the pumping the energy from a *dc* source into the travelling electromagnetic wave, generated by the moving lattice. Due to the deformation of the the moving lattice induced by interaction with the boundaries,[40] the I-V characteristics in this regime can be calculated only numerically. Below we present the main steps of a calculation (see Ref. 40 for details) as well as a comparison with the experiment. We will consider here only the main flux-flow branch corresponding to the case of uniformly sliding triangular lattice. The termination point of this branch is related to instability of the moving triangular vortex lattice.[40,41] The high-voltage branches in the JFF regime are apparently related with more complicated behavior and beyond the scope of this paper. We emphasize that at high velocity, when the washboard frequency exceeds the inverse quasiparticle relaxation time, one has to take into account the frequency dependence of the quasiparticle conductivity[17] which leads to the renormalization of the plasma frequency and Swihart velocity.

At high fields in the resistive state the interlayer phase differences depend approximately linearly on coordinate and time

$$\theta_n(t,x) \approx \omega_E t + k_H x + \phi_n, \tag{4}$$

where ω_E is the Josephson frequency and k_H is magnetic wave vector. In the following we will use reduced parameters: $\omega_E \to \omega_E/\omega_p$, $k_H \to k_H \gamma s$ (see Table 1). The most important degrees of freedom in this state are the phase shifts ϕ_n, which describe the structure of the moving Josephson vortex lattice. In particular, for the static triangular lattice $\phi_n = \pi n$. The lattice structure experiences a nontrivial evolution with increase of velocity. The equations for ϕ_n can be derived from the coupled sine-Gordon equations for $\theta_n(t,x)$ by expansion with respect to the Josephson current and averaging out fast degrees of freedom.[40] In the case of a steady state for a stack consisting of N junctions, this gives the following set of equations

$$\frac{1}{2}\sum_{m=1}^{N} \mathrm{Im}\left[\mathcal{G}(n,m)\exp\left(i\left(\phi_m - \phi_n\right)\right)\right] = i_J, \tag{5}$$

where $n = 1, 2 \ldots N$ and $i_J \equiv i_J(k_H, \omega_E) = \langle \sin\theta_n(t,x)\rangle$ is the reduced Josephson current, which has to be obtained as a solution of these equations. The complex function $\mathcal{G}(n,m)$ describes phase oscillations in the m-th layer excited by the oscillating Josephson current in the n-th layer. For a finite system it consists of the bulk term $G(n-m)$ plus the top and bottom reflections (multiple reflections can be neglected):

$$\mathcal{G}(n,m) = G(n-m) + \mathcal{B}G(n+m) + \mathcal{B}G(2N+2-n-m),$$

where

$$\begin{aligned} G(n) &= \int \frac{dq}{2\pi}\frac{\exp(iqn)}{\omega^2 - i\nu_c\omega - \Omega^2(k,q,\omega)}, \\ \Omega^2(k,q,\omega) &= \frac{k^2\left(1+i\nu_{ab}\omega\right)}{2(1-\cos q) + \left(1+i\nu_{ab}\omega\right)/l^2} \end{aligned} \tag{6}$$

$\omega = \omega_E$ and $k = k_H$ are the frequency and the in-plane wave vector of the travelling electromagnetic wave generated by moving lattice. The real and imaginary parts of $\Omega^2(k,q,\omega)$ give the spectrum of the collective plasma oscillations and their dumping due to in-plane quasiparticle dissipation (in reduced units). The dissipation parameters, ν_c and ν_{ab}, and reduced penetration depth l are defined in Table 1. $\mathcal{B} = \mathcal{B}(k,\omega)$ is the amplitude of reflected electromagnetic wave. For the practical case of the boundary between the static and moving Josephson

lattices a detailed calculation of $\mathcal{B}(k,\omega)$ is presented in Ref. 40.

In general, the quasiparticle conductivities in the definitions of ν_c and ν_{ab} are the complex conductivities at the Josephson frequency. The frequency dependence is especially important for the in-plane conductivity. The maximum Josephson frequency at the termination point of the flux-flow branch exceeds the value $1/\tau$ at fields $B \gtrsim 2$ T. Therefore the frequency dependence has to be taken into account. We use the Drude-like frequency dependence of $\nu_{ab} \equiv \nu_{ab}(\omega)$:

$$\nu_{ab}(\omega) = \frac{\nu_{ab0}}{1 + i\omega\tau} \tag{7}$$

where τ is the quasiparticle relaxation time. The solution of Eq. (5) yields the current-voltage characteristic

$$j(E_z) = \sigma_c E_z + J_c\, i_J(k_H, \omega_E),$$

where k_H and ω_E has to be expressed via magnetic and electric fields (see Table 1).

We solved Eqs. (5) numerically and calculated the I-V dependencies for the first flux-flow branch. We used σ_c and σ_{ab}/γ^4 obtained from the fit of $\rho_{ff}(B)$, assumed $\lambda_{ab} = 200$ nm, and adjusted γ to obtain the I-V dependencies most close to experimental ones. The results are shown in Fig. 8 for two values of magnetic field, $B = 1$ T and $B = 2$ T at $T = 4.2$ K. One can see a very reasonable fit to experiment for both field values using $\gamma \approx 500$. At high fields (see curves at 2 T) we found the fit can be significantly improved by taking into account frequency dependence of σ_{ab} via Eq. (7). The best approximation here was found for $1/(2\pi\tau) = 0.6$ THz. Both fitting parameters found to be quite reasonable. The value for γ is consistent with the typical value of $J_c(0)$ for our samples at low temperatures, $J_c(0) = 1 - 2$ A/cm^2, while the value of $1/(2\pi\tau)$ is consistent with the microwave data of Corson *et al.*[17] where the relaxation rate at low temperature was found to be ≈ 1 THz.

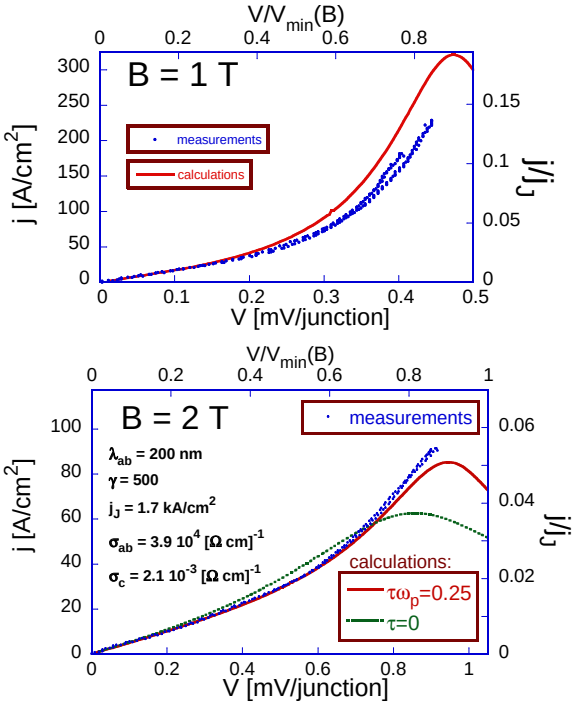


FIG. 8: Comparison of the experimental I-V characteristics measured on long BSCCO stack at fields $B = 1$T and $B = 2$T at 4.2 K with calculated numerically using Eq. (5). For both cases γ was used as a fitting parameter. The best fit was found at $\gamma = 500$. For the I-V characteristic at B=2 T also τ has been varied. The best fit was found at $\omega\tau = 0.25$. For such relaxation rate frequency dependence of σ_{ab} have very weak influence on the I-V shape at 1 T. In the upper axes the voltage scale $V_{\min}(B) \equiv Bs^2/(2\lambda_{ab}\sqrt{\epsilon}) \sim 0.5$ mV/T corresponds to the voltage at which the lattice velocity reaches the minimum velocity of electromagnetic wave $sc/(2\lambda_{ab}\sqrt{\epsilon})$. The parameters assumed in calculations are listed in the lower plot.

C. Renormalization of Swihart velocity by quasiparticles

Relatively low quasiparticle relaxation rates lead to an important observable consequence: renormalization by quasiparticles of the Swihart velocity at high frequencies, $\omega > 1/\tau$. The Swihart velocity is the in-plane velocity of the electromagnetic wave at the maximum c-axis wave vector, $k_z = \pi/s$. For this mode, out-of-phase oscillations of c-axis current in the neighboring layers induce oscillations of the in-plane current leading to strong coupling with the in-plane charge transport. As a consequence, the velocity of this mode, $cs/(2\lambda_{ab}\sqrt{\epsilon})$, is strongly reduced by the Cooper pairs in comparison with velocity of the transverse electromagnetic wave, $c/\sqrt{\epsilon}$. At small frequencies the in-plane motion of quasiparticles only contributes to the dissipation. However, when frequency exceeds the scattering rate, quasiparticles contribute to the inductive response in the same way as the superconducting electrons do, reducing an effective screening length and increasing the Swihart velocity. We will analyze this effect quantitatively. The spectrum of the plasma mode, $\omega_p = \omega_p(k,q)$ and its damping parameter $\nu = \nu(k,q)$ are determined by the equation (reduced units) $\omega_p^2 + i\nu\omega_p = i\nu_c\omega_p + \Omega^2(k,q,\omega_p)$ with $\Omega(k,q,\omega_p)$ defined by Eq. (6), i.e., $\omega_p(k,q)$ is given by the solution of the equation

$$\omega_p^2 = \mathrm{Re}[\Omega^2(k,q,\omega_p)]$$

For the minimum frequency at fixed k corresponding to $q = \pi$ we obtain

$$\omega_p^2 \approx \frac{k^2}{4}\left(1 + \mathrm{Re}\left[\frac{\nu_{ab} i\omega_p}{1 + i\tau\omega_p}\right]\right)$$

From this equation one can easily observe that the Swihart velocity $c_s = \omega_p/k$ (in units of $sc/(\lambda_{ab}\sqrt{\epsilon})$) has two simple asymptotics

$$c_s = \begin{cases} 1/2, \text{ at } c_s k\tau \ll 1 \\ \sqrt{1 + \nu_{ab}/\tau}/2, \text{ at } c_s k\tau \gg 1 \end{cases}$$

The physical meaning of the quasiparticle renormalization factor $r = \sqrt{1+\nu_{ab}/\tau}$ becomes more transparent if we transfer to the real units and use the two-fluid expressions for λ_{ab} and σ_{ab}, $\lambda_{ab}^2 = m_{ab}c^2/(4\pi n_s e^2)$, $\sigma_{ab} = n_n\tau e^2/m_{ab}$. Then the renormalization factor reduces to $\nu_{ab}/\tau = n_n/n_s$ and

$$c_s = \begin{cases} \sqrt{\pi s^2 n_s e^2/\varepsilon m_{ab}}, \text{ at } c_s k\tau \ll 1 \\ \sqrt{\pi s^2 \left(n_s+n_n\right) e^2/\varepsilon m_{ab}}, \text{ at } c_s k\tau \gg 1 \end{cases}$$

i.e., the renormalization amounts to replacement of the superfluid density n_s by the total density $n_s + n_n$.

The first flux-flow branch terminates due to instability of the triangular lattice configuration at the velocity close to the Swihart velocity.[40,41] Therefore, the Swihart velocity can be estimated from the voltage at the endpoint of the first flux-flow branch. As a consequence of quasiparticle renormalization, one can expect an increase of the maximum voltage for the first flux-flow branch when the Josephson frequency at this voltage exceeds $1/\tau$. The estimate of the renormalization factor for our samples for $\omega_p\tau = 0.25$, $\lambda_{ab} = 0.2$ μm, $\sigma_{ab} = 4\cdot 10^4$ $(\Omega$ cm$)^{-1}$ gives the value $r = 2$. Experimentally, the Swihart velocity can be extracted from the slope of the linear dependence of the maximum flux-flow voltage on the magnetic field, $V_{ffmax}(H)/H$. We found (see also Ref. 30), that the slope increases at magnetic fields above 1.5 T (Fig. 5). That field corresponds to the washboard frequency about 0.5 THz, which is very close to the quasiparticle relaxation rate. Therefore, the increase of the slope of $V_{ffmax}(H)$ at higher frequencies may be interpreted as an increase of the Swihart velocity due to a renormalization of plasma frequency at $\omega > 1/\tau$. Experimentally, the slope of $V_{ffmax}(H)$ increases by factor 2.1 that is very close to the theoretical estimate of the renormalization factor.

IV. CONCLUSIONS

In summary, we carried out detailed experimental and theoretical studies of the linear and non-linear Josephson flux-flow regimes in BSCCO. Both regimes as shown can be well described by the developed theoretical model. That takes into account an additional channel in the dissipation related to the *ac* in-plane quasiparticle currents accompanying JFF. The criterion of the applicability of the model $\sigma_{ab}/(\sigma_c\ \gamma^2) > 1$ is shown to be valid in a wide temperature range below T_c. From the measurements in the linear JFF regime we extracted the values of both components of the quasiparticle conductivity at low frequency limit. The extracted temperature dependence $\sigma_{ab}(T)$ is consistent with the microwave measurements, while $\sigma_c(T)$ reproduces the *dc* measurements on small mesas in zero magnetic field. The fit of the data measured in the nonlinear regime to the theoretical model allowed us to estimate quasiparticle relaxation time τ and the renormalized Swihart velocity at high frequency limit $\omega\tau > 1$. All these results demonstrate the applicability of JFF measurements for studies of quasiparticle dynamics in layered high-T_c superconductors.

We derived from the experimental data for $\sigma_c(T)$ the impurity bandwidth γ_i and from the nonlinear part of the *I-V* characteristics we estimated the QPs relaxation rate $1/\tau$, which is consistent with γ_i. In a similar way, the universality of $\sigma_{00}^{(c)}$ may be checked by measurements of pristine and irradiated crystals and upper limit for Ω_0 may be given by study of $\sigma_c(T)$ at lower temperatures and frequencies.

V. ACKNOWLEDGEMENTS

We would like to thank N. Pedersen and A. Ustinov, for fruitful discussions, M. Graf and K. Gray for critical reading of the manuscript and constructive comments, V. N. Pavlenko for technical assistance, and T. Yamashita for support of this work. YIL acknowledges support from the CRDF grant No. RP-12397-MO-02 and grant from Russian Ministry of Science and Industry No. 40.012.1.111.46. In Argonne this work was supported by the U. S. DOE, Office of Science, under contract No. W-31-109-ENG-38. AEK and YIL acknowledge support from the NATO Travel grant No. PST.CLG.979047.

[1] A. Kaminski, J. Mesot, H. Fretwell, J. C. Campuzano, M. R. Norman, M. Randeria, H. Ding, T. Sato, T. Takahashi, T. Mochiku, K. Kadowaki, and H. Hoechst, Phys. Rev. Lett. **84**, 1788 (2000); T. Valla, A. V. Fedorov, P. D. Johnson, Q. Li, G. D. Gu, and N. Koshizuka , Phys. Rev. Lett. **85**, 828 (2000).

[2] L. P. Gorkov and P. A. Kalugin, Pis'ma Zh. Eksp. Teor. Fiz. **41**, 208 (1985) [JETP Lett. **41**, 253 (1985)].

[3] P. A. Lee, Phys. Rev. Lett. **71**, 1887 (1993).

[4] A. V. Balatsky, A. Rosengren, and B. L. Altshuler, Phys. Rev. Lett. **73**, 720 (1994).

[5] P. J. Hirschfeld, W. O. Putikka, and D. J. Scalapino, Phys. Rev. B, **50**, 10250 (1994).

[6] Y. Sun and K. Maki, Europhys. Lett. **32**, 355 (1995).

[7] M. J. Graf, S.-K. Yip, J. A. Sauls, and D. Rainer, Phys. Rev. B **53**, 15 147 (1996).

[8] D. Xu, S. K. Yip, and J. A. Sauls, Phys. Rev. B **51**, 16 233 (1995); A. J. Millis, S. M. Girvin, L. B. Ioffe, and A. I. Larkin, J. Phys. Chem. Solids **59**, 1742 (1998).

[9] A. C. Durst and P. A. Lee, Phys. Rev. B, **62**, 1270 (2000)

[10] D. A. Bonn, P. Dosanjh, R. Liang, and W. N. Hardy, Phys. Rev. Lett. **68**, 2390 (1992); D. A. Bonn, S. Kamal, K. Zhang, R. Liang, D. J. Baar, E. Klein, and W. N. Hardy, Phys. Rev. B **50**, 4051 (1994); A. Hosseini, R. Harris, S.

Kamal, P. Dosanjh, J. Preston, R. Liang, W. N. Hardy, and D. A. Bonn, Phys. Rev. B **60**, 1349 (1999).
[11] Yu. I. Latyshev, T. Yamashita, L. N. Bulaevskii, M. J. Graf, A. V. Balatsky, and M. P. Maley, Phys. Rev. Lett. **82**, 5345 (1999).
[12] P. J. Hirschfeld and W. O. Putikka, Phys. Rev. Lett. **77**, 3909 (1996).
[13] A. Altland, B. D. Simons, M. R. Zirnbauer, Physics Reports **359**, 283 (2002)
[14] W. A. Atkinson, P. J. Hirschfeld, and A. H. MacDonald, Phys. Rev. Lett. **85**, 3922 (2000); W. A. Atkinson, P. J. Hirschfeld, A. H. MacDonald, and K. Ziegler Phys. Rev. Lett. **85**, 3926 (2000).
[15] Shih-Fu Lee, D. C. Morgan, R. J. Ormeno, D. M. Broun, R. A. Doyle, J. R. Waldram, and K. Kadowaki Phys. Rev. Lett. **77**, 735 (1996); H. Kitano, T. Hanaguri, Y. Tsuchiya, K. Iwaya, R. Abiru, and A. Maeda J. Low Temp. Phys. **117**, 1241 (1999).
[16] H. J. Fink and M. R. Trunin, Phys. Rev. B 62, 3046 (2000).
[17] J. Corson, J. Orenstein, S. Oh, J. O'Donnell, and J. N. Eckstein, Phys. Rev. Lett. **85**, 2569 (2000).
[18] D. B. Romero, C. D. Porter, D. B. Tanner, L. Forro, D. Mandrus, L. Mihaly, G. L. Carr, and G. P. Williams Phys. Rev. Lett. **68**, 1590 (1992)
[19] D. N. Basov, R. Liang, D. A. Bonn, W. N. Hardy, B. Dabrowski, M. Quijada, D. B. Tanner, J. P. Rice, D. M. Ginsberg, and T. Timusk, Phys. Rev. Lett. **74**, 598 (1995).
[20] A. F. Santander-Syro, R. P. S. M. Lobo, N. Bontemps, Z. Konstantinovic, Z. Li, and H. Raffy, Phys. Rev. Lett. **88**, 097005 (2002)
[21] R. Movshovich, M. A. Hubbard, M. B. Salamon, A. V. Balatsky, R. Yoshizaki, J. L. Sarrao, and M. Jaime, Phys. Rev. Lett., **80** 1968 (1998).
[22] S. Nakamae, K. Behnia, L. Balicas, F. Rullier-Albenque, H. Berger, and T. Tamegai, Phys. Rev. B **63**, 184509 (2001).
[23] K. Krishana, J. M. Harris, and N. P. Ong, Phys. Rev. Lett. **75**, 3529 (1995); B. Zeini, A. Freimuth, B. Bchner, M. Galffy, R. Gross, A. P. Kampf, M. Klser, G. Mller-Vogt and L. Winkler, Eur. Phys. J. B **20**, 189 (2001).
[24] A. E. Koshelev, Phys.Rev. B **62**, R3616 (2000).
[25] L. N. Bulaevskii and J. R. Clem, Phys. Rev. B, **44**, 10234 (1991).
[26] L. N. Bulaevskii, D. Domingez, M. P. Maley, A. R. Bishop, and B. I. Ivlev, Phys. Rev. B 53, 14601 (1996).
[27] M. Tinkham, *Introduction to Superconductivity*, McGraw-Hill, 1996.
[28] as a review, see A. Barone and G. Paterno, *Physics and Applications of the Josephson Effect*, Wiley, New York, 1982.
[29] J. U. Lee, J. E. Nordman, and G. Hohenwarter, Appl. Phys. Lett., **67**, 1471 (1995); J. U. Lee, P. Guptasarma, D. Hornbaker, A. El-Kortas, D. Hinks, and K. E. Gray, Appl. Phys. Lett., **71**, 1412 (1997)
[30] G. Hechtfischer, R. Kleiner, A. V. Ustinov, and P. Müller Phys. Rev. Lett. **79**, 1365 (1997); G. Hechtfischer, R. Kleiner, K. Schlenga, W. Walkenhorst, P. Müller, and H. L. Johnson Phys. Rev. B, **55**, 14638 (1997)
[31] Yu. I. Latyshev, P. Monceau, and V. N. Pavlenko, Physica C, **282-287**, 387 (1997); Physica C, **293**, 174 (1997).
[32] Yu. I. Latyshev, I. G. Gorlova, A. M. Nikitina, V. U. Antokhina, S. G. Zybtsev, N. P. Kukhta, and V. N. Timofeev, Physica C, **216** 471(1993).
[33] Yu. I. Latyshev, S.-J. Kim, and T. Yamashita, IEEE Trans. on Appl. Supercond. **9**, 4312(1999).
[34] T. Watanabe, T. Fujii, and A. Matsuda, Phys. Rev. Lett. **79** (1997) 2113.
[35] R. Kleiner, F. Steinmeyer, G. Kunkel, and P. Müller, Phys. Rev. Lett. **68**, 2394 (1992); R. Kleiner and P. Müller, Phys. Rev. B, **49**, 1327 (1994).
[36] The same result was obtained earlier in Ref. 26, Eq. (42), but with a misprint in the sign in front of the term with σ_{ab}, where plus should stay.
[37] W. E. Lawrence and S. Doniach, in Proceedings of the 12^{th} Intern. Conference on Low Temperature Physics, Kyoto, Japan, 1971, ed. by E. Kanda (Keigaku,Tokyo,1971), p. 361.
[38] T. Jacobs, S. Sridhar, Q. Li, G. D. Gu, and N. Koshizuka, Phys. Rev. Lett. **75**, 4516 (1995).
[39] M. B. Gaifullin, Y. Matsuda, N. Chikumoto, J. Shimoyama, K. Kishio, and R. Yoshizaki, Phys. Rev. Lett. **83**, 3928 (1999).
[40] A. E. Koshelev and I. S. Aranson, Phys. Rev. Lett. **85**, 3938 (2000); Phys. Rev. B **64**, 174508 (2001).
[41] S. N. Artemenko and S. V. Remizov, Phys. Rev. B **67**, 144516 (2003).

Table 1. Meanings, definitions and practical formulas for the reduced parameters used in the paper. In practical formulas $f_p = \omega_p/2\pi$ means plasma frequency, ρ_c and ρ_{ab} are the components of the quasiparticle resistivity

Notation	Meaning	Definition(CGS)	Practical formula (BSCCO)
ω_E	reduced Josephson frequency	$\frac{2\pi csE_z}{\Phi_0\omega_p}$	$\frac{U[\mathrm{mV/junction}]}{2{\cdot}10^{-3}f_p[\mathrm{GHz}]}$
k_H	magnetic wave vector	$\frac{2\pi H\gamma s^2}{\Phi_0}$	
ν_c	c-axis dissipation parameter	$\frac{4\pi\sigma_c}{\varepsilon_c\omega_p}$	$\frac{1.8{\cdot}10^3}{\varepsilon_c\rho_c[\Omega{\cdot}\mathrm{cm}]f_p[\mathrm{GHz}]}$
ν_{ab}	in-plane dissipation parameter	$\frac{4\pi\sigma_{ab}\lambda_{ab}^2\omega_p}{c^2}$	$\frac{0.79(\lambda_{ab}[\mu m])^2 f_p[\mathrm{GHz}]}{\rho_{ab}[\mu\Omega{\cdot}\mathrm{cm}]}$
l	reduced London penetration depth	λ_{ab}/s	